Int. J. Heat Mass Transfer. Vol. 22, pp. 1021–1032
Pergamon Press Ltd. 1979. Printed in Great Britain

THE EFFECT OF DEFORMATION AND THERMOSET CURE ON HEAT CONDUCTION IN A CHOPPED-FIBER REINFORCED POLYESTER DURING COMPRESSION MOLDING

M. R. BARONE and D. A. CAULK
Engineering Mechanics Department, General Motors Research Laboratories,
Warren, Michigan 48090, U.S.A.

(*Received* 26 *July* 1978)

Abstract—This paper concerns heat conduction in a chopped-fiber reinforced polyester resin during compression molding of thin sheet-like parts. Since the resin generates heat as it cures, the general boundary value problem involves a deforming heat conductor which reacts chemically. The randomly woven fiber structure in the sheet molding compound (SMC) motivates a kinematical assumption on the material deformation in the mold cavity. The resulting description of the deformation field is then used to formulate a boundary value problem for the temperature distribution in the deforming SMC in terms of coordinates that move with the material. From the solution to this problem we derive a general expression in closed form for the nonuniform distribution of heat energy absorbed from the mold surface as each part is molded. The exothermic cure reaction in the polyester resin, which begins after the mold closes, is characterized in terms of heat generated in the SMC. Numerical analysis of the transient distribution of temperature and cure shows how the degree of coupling between heat conduction and cure depends on the thickness of the molded sheet. The results of the analysis also determine the effect of sheet thickness and mold temperature on cure time, subject to limitations of thermal degradation.

NOMENCLATURE

a_1, a_2, b_1, b_2,	kinetic coefficients;
c,	heat capacity (per unit mass);
e,	heat flux integral (see 4.12);
f,	function defined by (4.8);
k_1, k_2,	components of conductivity;
l,	position of mold surface;
l_f,	final position of mold surface;
$l_i(x,y)$,	mold position when charge front first reaches the point (x,y);
l_0,	initial position of mold surface;
m,n,	kinetic exponents;
q,	heat flux at mold surface;
Q,	heat evolved by cure reaction;
$\dot{Q}_I$,	rate of heat supplied to sample by DSC;
Q_T,	total heat of reaction during cure;
R,	universal gas constant;
s,	constant mold-closing speed;
t,	time;
t_f,	time it takes the mold to close;
$t_i(x,y)$,	time when charge front first reaches the point (x,y);
T,	absolute temperature;
T_m,	absolute mold temperature;
T_0,	initial absolute temperature of charge;
u,v,w,	velocity components;
x,y,z,	Cartesian coordinates.

Greek symbols

α,	degree of cure;
θ,	temperature increase in SMC;
θ_0,	initial difference between mold temperature and charge temperature;
$\hat{\theta}$,	temperature in undeformed SMC (see 6.1);
κ_1,	transverse thermal diffusivity;
ξ,η,ζ,	convected coordinates;
ρ,	density;
τ,	shifted time scale;
ϕ,	mold displacement function.

Dimensionless parameters

F,	Fourier number;
$\hat{T}$,	absolute temperature;
ν,	ratio of time scales (see 7.4);
σ,	time.

1. INTRODUCTION

IN RECENT years, the use of composite materials has expanded from aerospace applications to consumer product industries. Many consumer products, unlike those in aerospace, must be produced in large volume and at relatively low unit costs. The resulting need for efficient manufacturing processes poses new technical problems which are unique to mass production.

Our interest here is in compression molding of a filled polyester resin reinforced by chopped glass fibers. The unmolded composite is produced in sheets which are typically 3 to 6 mm thick. The resin has the consistency of a thick dough and the chopped fibers (about 25 mm long) are randomly oriented in the plane of the sheet. In this form, the material is called sheet molding compound, or simply SMC. The composition of the SMC considered in this paper is given in Table 1.

Table 1. SMC composition

		Percent by weight
Resin:		27.35
Unsaturated polyester	10.50	
Low shrink additive	3.45	
Styrene monomer	13.40	
Filler (Calcium carbonate)		40.70
Thickener (Magnesium oxide)		0.70
Initiator		0.25
Lubricant (Zinc stearate)		1.00
Glass Fibers (25 mm long)		30.00
		100.00

In the compression molding process, a number of SMC sheets are cut to a desired shape and then stacked on one face of the mold to form the charge (see Fig. 1). As the mold closes, the charge deforms to fill the mold cavity and the resulting part is heated by contact with the warm mold until an exothermic cross-linking reaction takes place in the polymer resin. The heat evolved by the reaction is conducted into the mold halves as the polymer cures to a solid. After the part has cured sufficiently, the mold can be opened and the finished part removed.

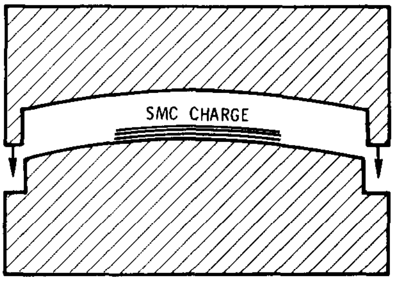

Fig. 1. Schematic illustration of the compression molding process.

Because of the high cost of compression molding equipment, cycle time is a critical economic factor in high volume production. Short cycle time, however, can give rise to two problems involving heat transfer. The first concerns rapid recovery of uniform temperature on the mold surface after each part is molded, and the second involves nonuniform, nonisothermal cure in some parts due to strong coupling of heat conduction with the exothermic cure reaction.

Although the mold surface is usually cooled very little during molding of a single part, the flow of SMC in the mold cavity causes this cooling to occur nonuniformly, and unless the mold surface can return to a uniform temperature before the next cycle begins, heat will be depleted from certain areas of the mold after a number of parts have been molded. As the mold temperature drops, the part takes longer to cure, and this increases cycle time. Eventually a steady-state is reached, but if the mold recovery is slow, the steady-state cycle time may be unacceptably long. To avoid this problem, the mold can be selectively heated in accordance with the nonuniform depletion caused by the deformation. Such an approach requires a detailed account of the heat transfer to the deforming SMC as it flows in the mold cavity.

If the thermal recovery of the mold can be made sufficiently rapid, the bulk of the cycle time will be consumed in curing the part after the mold is closed. To shorten this part of the cycle, the polyester resin is usually formulated for a rapid rate of cure. But rapid cure can result in a reaction time scale comparable to the time scale of thermal diffusion in typical parts. When this occurs, the progressing cure reaction may couple with heat conduction, causing nonuniform cure in the part. This coupling can also cause excessively high temperatures during cure, giving rise to thermal degradation of the resin and residual stresses caused by differential thermal shrinkage. Analysis of the cure process can identify when such problems exist and guide the engineer in implementing appropriate design modifications.

In this paper, we address the above problems by analyzing heat conduction in the SMC as it deforms in the mold cavity and subsequently cures to a solid. Although the SMC is heated somewhat as the mold closes, the cure reaction of the polyester resin is initially so slow that nearly all curing (and therefore heat generation) takes place *after* the mold has closed. We therefore divide the total problem into two parts: (1) Analysis of heat conduction in the deforming compound as the mold closes and when the heat generation of cure can be neglected; and (2) analysis of the coupled problem of heat conduction and cure after the mold closes and when the material no longer deforms. After a preliminary discussion of material idealizations in Section 2, we formulate and solve the first part of the problem in Sections 3 and 4. The cure kinetics of the polyester resin are then characterized in Section 5 and the second part of the problem is treated in Sections 6–8.

2. MATERIAL IDEALIZATIONS

Because the fiber structure of SMC strongly influences its deformation during molding, we begin with a description of the process by which the fibers and resin are combined to form SMC.

In a typical process, continuous glass-fiber rovings are chopped to lengths of about 25 mm and these cascade with random orientation onto a moving layer of resin supported by a polyethylene sheet. This operation forms the loose fiber weave pictured in Fig. 2. Downstream, another layer of resin is rolled on top of the fibers and the resulting sandwich is compressed between a series of rollers to expel air and impregnate the fiber mat with the resin.

Strictly speaking, a general description of the deformation in SMC during molding should account for relative motion between the resin and fibers. However, since the filled polyester resin is highly viscous, this relative motion is likely to be small compared to the bulk motion of the deforming compound and is therefore neglected in this analysis. Moreover since the average fiber spacing is usually small relative to the smallest dimension of the molded part, we can smear the resin and fiber constituents and represent the SMC as a single phase continuum. In addition, the fibers are assumed to be uniformly distributed so that the continuum may be regarded as homogeneous.

The length of the chopped fiber rovings is not small relative to part thickness and so their preferred orientation in the resin matrix can induce material anisotropy. Since the fibers are randomly oriented in the plane of the sheet, this anisotropy is characterized by a single preferred direction perpendicular to the plane of the sheet. It follows that the thermal conductivity of the SMC can be characterized by a transverse component k_1 and an in-plane component k_2. Because 70% of the compound by weight is chemically inert (see Table 1), we assume that k_1 and k_2 do not vary as the resin cures. Similarly, the density ρ and heat capacity c of the SMC are also assumed to be constant. Values for these properties were measured from samples of cured material at temperatures ranging from 25 to 150°C. These measurements showed little variation with temperature and yielded the following average results:

$$\rho = 1900\,\mathrm{kg \cdot m^{-3}}, \qquad c = 1.0\,\mathrm{J \cdot g^{-1} \cdot K^{-1}},$$
$$k_1 = 0.53\,\mathrm{W \cdot m^{-1} \cdot K^{-1}}, \; k_2 = 0.61\,\mathrm{W \cdot m^{-1} \cdot K^{-1}}. \tag{2.1}$$

3. KINEMATICS OF THE DEFORMATION

Qualitative description

In general, the charge is made up of a number of SMC sheets stacked on top of each other. Within each sheet, the interlocking fiber weave (Fig. 2) resists transverse shear deformation so that when the mold closes, the shear is confined to the surfaces between sheets. Consequently, the individual sheets stretch independently with the hotter, outer sheets experiencing greater deformation. This behavior was observed experimentally by Marker and Ford [1] in thick charges consisting of about ten layers of SMC. Because thin sheet construction is attractive in automotive structural panels [2], we restrict attention in this analysis to thinner charges consisting of one (or at most two) layers of SMC. In this case, the interlocking fiber weave (Fig. 2) should strongly resist transverse shearing everywhere in the flow region. Although the entangled fibers resist transverse shearing, their relatively short length cannot

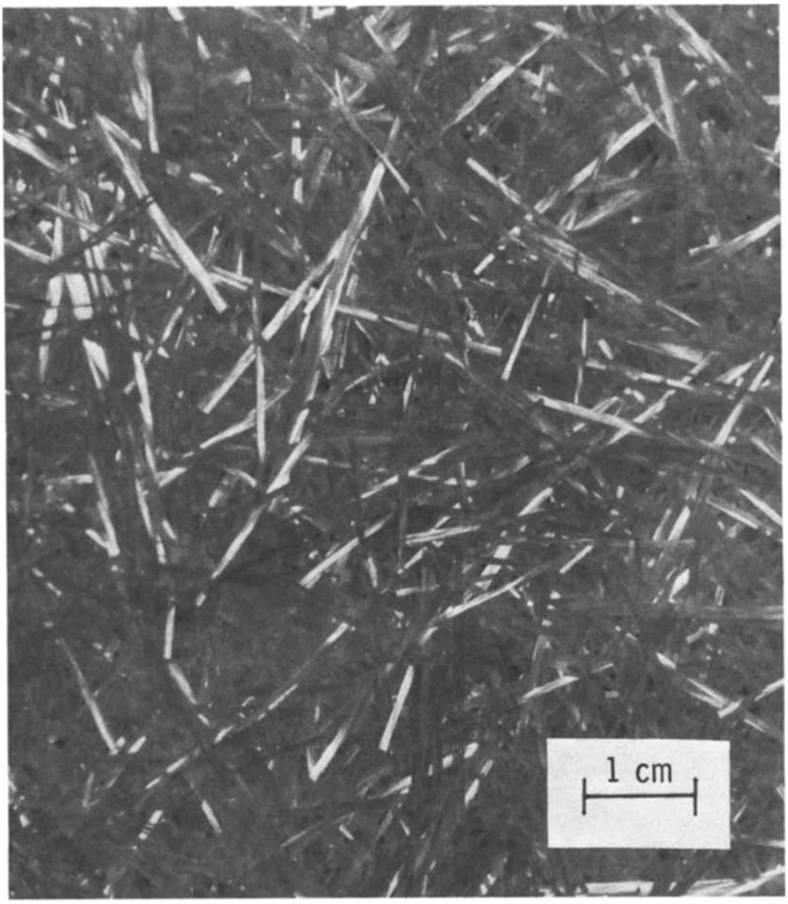

FIG. 2. Fiber weave.

prevent the weave from pulling apart, and so they offer considerably less resistance to extensional deformation of the sheet.

Formulation

Consider rectangular Cartesian coordinates (x,y,z), with the z-axis parallel to the direction of mold motion, and let (u, v, w) be the corresponding components of velocity in the SMC. We confine attention to parts which are symmetric with respect to their midplane (say $z = 0$) and let the equation

$$z = \pm l(x, y, t) \tag{3.1}$$

define the position of the mold surfaces relative to this plane. Since the mold translates parallel to the z-axis, the function $l(x, y, t)$ can be decomposed in the form:

$$l(x, y, t) = l_0(x, y) - \phi(t). \tag{3.2}$$

We call $\phi(t)$ the *mold displacement function* and let $t = 0$ when the mold surface first makes full contact with the charge so that $\phi(0) = 0$. Then $z = l_0(x, y)$ defines the initial position of the mold surface. For later reference we also assume that l_0 is a smooth and slowly varying function of x and y.

Motivated by the earlier description of the deformation during molding, we assume that the interlocking fiber weave so constrains the motion of the SMC that the velocity components u and v satisfy

$$\partial u/\partial z = \partial v/\partial z = 0. \tag{3.3}$$

In addition, the material is assumed to be incompressible so that

$$\partial u/\partial x + \partial v/\partial y + \partial w/\partial z = 0. \tag{3.4}$$

Differentiating (3.4) with respect to z and imposing the condition (3.3) yields

$$\partial^2 w/\partial z^2 = 0. \tag{3.5}$$

This equation can be integrated in the form:

$$w(x, y, z, t) = a(x, y, t)z + b(x, y, t). \tag{3.6}$$

From symmetry we have

$$w(x, y, 0, t) = b(x, y, t) = 0. \tag{3.7}$$

Also, the kinetic boundary condition at the mold surface $z = l$ is

$$w(x, y, l, t) = \dot{l} = -\dot{\phi} + u\frac{\partial l_0}{\partial x} + v\frac{\partial l_0}{\partial y}, \tag{3.8}$$

where the superposed dot denotes the material time derivative. Substituting (3.7) and (3.8) into (3.6) gives

$$a(x, y, t) = \dot{l}/l. \tag{3.9}$$

With (3.7) and (3.9) the velocity (3.6) reduces to

$$w(x, y, z, t) = \dot{z} = z\frac{\dot{l}}{l}, \tag{3.10}$$

which may be integrated to yield

$$\frac{z}{l} = \text{constant}. \tag{3.11}$$

The constant (3.11) depends on the material particle, and without loss in generality can be identified with the convected (or material) coordinate ζ. Then (3.11) becomes

$$z = \xi l. \tag{3.12}$$

The general expression for the velocity field in the x–y plane follows directly from (3.3):

$$\dot{x} = u(x, y, t), \quad \dot{y} = v(x, y, t). \tag{3.13}$$

Now let the remaining convected coordinates (ξ, η) be identified with the (x, y) position of a material particle at $t = 0$. Then the deformation field corresponding to (3.13) can be written as

$$x = x(\xi, \eta, t), \quad y(\xi, \eta, t). \tag{3.14}$$

Equations (3.14) and (3.12) represent the most general deformation consistent with the assumption (3.3) and the symmetry condition (3.7). Since the deformation (3.14) in the x–y plane is decoupled from that (3.12) along the z-axis, the deforming charge can be viewed as an assemblage of material filaments (identified by the coordinates ξ and η) which always remain parallel to the z-axis. Their length

$$l(\xi, \eta, t) = l(x(\xi, \eta, t), y(\xi, \eta, t), t), \tag{3.15}$$

changes as the mold closes.

4. HEAT CONDUCTION IN THE DEFORMING COMPOUND

Let the initial temperature of the mold surface be spatially uniform. Then since the conductivity of the steel mold ($\sim 33\,\mathrm{W \cdot m^{-1} \cdot K^{-1}}$) is so much larger than that of the SMC (2.1), we assume that the temperature at the mold surface remains constant and uniform, even after it contacts the SMC. In terms of the convected coordinates (ξ, η, ζ) introduced in Section 3, this assumption may be stated as

$$\frac{\partial \theta}{\partial \xi} = \frac{\partial \theta}{\partial \eta} = 0, \text{ on } \zeta = \pm 1, \tag{4.1}$$

where for convenience we let θ denote the temperature in the SMC in excess of the initial charge temperature. Now since the thickness of the charge is usually small relative to its shortest in-plane dimension, we neglect the partial derivatives in (4.1) for all $-1 \leqslant \zeta \leqslant 1$. Combining this assumption with (3.12), the heat balance in the deforming SMC can be written as†

$$\rho c\dot{\theta} = \frac{k_1}{l^2}\frac{\partial^2 \theta}{\partial \zeta^2}[1 + O(l_x^2 + l_y^2, l_{xx} + l_{yy})], \tag{4.2}$$

---

†Since the chemical reaction is extremely slow in the early stages of cure (due to a chemical inhibitor in the resin formulation), the heat of reaction during the few seconds it takes to close the mold can be neglected.

where a subscripted variable denotes partial differentiation. Invoking the earlier assumption that $l_0(x, y)$ varies smoothly and slowly in x and y, we neglect the second term in brackets in (4.2) and write the complete boundary value problem as

$$l^2(\xi, \eta, t)\frac{\partial \theta}{\partial t} = \kappa_1 \frac{\partial^2 \theta}{\partial \zeta^2}, \tag{4.3}$$

$$\theta(\xi, \eta, \zeta, 0) = 0,$$

$$\frac{\partial \theta}{\partial \zeta}(\xi, \eta, 0, t) = 0, \quad \theta(\xi, \eta, 1, t) = \theta_0. \tag{4.4}$$

Here θ_0 is the difference between the mold temperature and the initial temperature of the charge, and κ_1 is the transverse thermal diffusivity defined by

$$\kappa_1 = \frac{k_1}{\rho c}. \tag{4.5}$$

The boundary value problem (4.3) to (4.4) differs from the corresponding problem for a rigid slab only in the non-constant coefficient $l^2(\xi, \eta, t)$ on the left-hand side of (4.3). Hence, this term carries the entire effect of the deformation when the problem is formulated in terms of convected coordinates. Since l is independent of ζ, the system (4.3) and (4.4) can be solved using separation of variables in ζ and t, holding ξ and η fixed. The resulting solution is

$$\theta/\theta_0 = 1 + 4\sum_{n=0}^{\infty} \frac{(-1)^{n+1}}{(2n+1)\pi} \exp[-a_n \kappa_1 f(\xi, \eta, t)] \cos\left[\frac{(2n+1)\pi}{2}\zeta\right], \tag{4.6}$$

where

$$a_n = \frac{(2n+1)^2\pi^2}{4}. \tag{4.7}$$

The function $f(\xi, \eta, t)$ is defined by

$$f(\xi, \eta, t) = \int_0^t \frac{\mathrm{d}t}{[l(\xi, \eta, t)]^2}, \tag{4.8}$$

where ξ and η are held fixed in the integration. The expression (4.6) represents the developing temperature distribution along the material filament designated by ξ and η.

To illustrate the explicit form of the general solution (4.6) in a specific example, we consider the special case where the mold faces are plane and parallel. For simplicity, we assume the mold closes at a constant rate $2s$, so that

$$l_0 = \text{const.}, \qquad \phi = st. \tag{4.9}$$

In this case l_0 is independent of ξ and η, and from (4.8)

$$f(t) = \frac{t}{l_0(l_0 - st)}. \tag{4.10}$$

Combining (4.10) and (4.6) gives

$$\theta/\theta_0 = 1 + 4\sum_{n=0}^{\infty} \frac{(-1)^{n+1}}{(2n+1)\pi} \exp\left[\frac{-a_n\kappa_1 t}{l_0(l_0 - st)}\right] \cos\left[\frac{(2n+1)\pi z}{2(l_0 - st)}\right]. \tag{4.11}$$

As expected, (4.11) reduces to the classical solution for a rigid slab [3, p. 100] when the mold velocity vanishes.

Returning now to the general development, we consider the total heat energy $e(x, y)$ per unit area that one site (x, y) on the mold surface gives up during mold-closing. If $q(x, y, t)$ denotes the heat flux from the mold at $z = l$, then

$$e(x, y) = \int_{t_i(x,y)}^{t_f} q(x, y, t)\,\mathrm{d}t, \tag{4.12}$$

where t_f is the time that the mold closes and $t_i(x, y)$ is the instant of time that the deforming front of the SMC charge first arrives at the point† (x, y) on the mold surface. We call $e(x, y)$ the *heat flux integral*. The heat flux q can be calculated from the temperature solution (4.6). With the help of the transformations $(3.14)_{1,2}$, q can be expressed in the form:

$$q(x, y, t) = 4k_1\theta_0 \frac{\partial}{\partial z}\left\{\sum_{n=0}^{\infty} \frac{(-1)^{n+1}}{(2n+1)\pi} \exp[-a_n\kappa_1 f(x, y, t)] \cos\left[\frac{(2n+1)\pi z}{2l}\right]\right\}_{z=l}. \tag{4.13}$$

Since the infinite series in (4.13) converges uniformly for $t \geq t_i > 0$, the order of differentiation and summation can be interchanged and (4.13) reduces to:

$$q(x, y, t) = 2k_1\theta_0 \sum_{n=0}^{\infty} \frac{1}{l(x, y, t)} \exp[-a_n\kappa_1 f(x, y, t)], \quad t \geq t_i > 0. \tag{4.14}$$

---

†It is convenient to deal with the spatial coordinates (x, y) when referring to points on the mold surface since the mold translates parallel to the z-axis.

Substituting (4.14) into (4.12), the heat flux integral can now be expressed as

$$e(x,y) = 2k_1\theta_0 \int_{t_i(x,y)}^{t_f} \left\{ \sum_{n=0}^{\infty} \exp[-a_n\kappa_1 f(x,y,t)] \right\} \frac{\mathrm{d}t}{l(x,y,t)}. \tag{4.15}$$

Again since the infinite series in (4.15) converges uniformly for $t \geqslant t_i > 0$, the expression for e becomes

$$e(x,y) = 2k_1\theta_0 \sum_{n=0}^{\infty} \int_{t_i(x,y)}^{t_f} \exp[-a_n\kappa_1 f(x,y,t)] \frac{\mathrm{d}t}{l(x,y,t)}, \quad t_i > 0. \tag{4.16}$$

It can be shown that (4.16) also holds in the limit $t_i(x,y) \to 0$, corresponding to points in the initial charge region.

The expression (4.16) involves no approximation beyond (4.3) and the basic assumptions made in Sections 2 and 3. It is valid for an arbitrary mold displacement function $\phi(t)$ (see 3.2) and for an arbitrary charge configuration. To explicitly evaluate the integrals in (4.16), the function $l(x, y, t)$ and details of the in-plane deformation field (3.14) must be specified.

In the special case where the part thickness is uniform, l and f are functions of time only and (4.16) reduces to

$$e(x,y) = 2k_1\theta_0 \sum_{n=0}^{\infty} \int_{t_i(x,y)}^{t_f} \exp[-a_n\kappa_1 f(t)] \frac{\mathrm{d}t}{l(t)}. \tag{4.17}$$

Note that the dependence on x and y in the expression for e now enters only through the integral limit $t_i(x,y)$. Since $t_i(x,y) = 0$ at every point in the initial charge region, the heat flux integral for uniform parts has the same value at each of these points. To evaluate the heat flux integral at points outside the charge region of uniform parts, we need only specify $\phi(t)$ and $t_i(x,y)$. As an example, consider the case of a constant mold closing speed, $2s$, where the functions $\phi(t)$, $l(t)$ and $f(t)$ are given by (3.2), (4.9) and (4.10). With these expressions and some manipulation, (4.17) becomes:

$$e(x,y) = -2\rho c\theta_0 l_0 F \times \sum_{n=0}^{\infty} \left[\exp(a_nF)E_1\left(a_nF\frac{l_0}{l}\right) \right]_{l_i(x,y)}^{l_f}, \tag{4.18}$$

where F is defined by

$$F = \frac{\kappa_1}{l_0 s}, \tag{4.19}$$

and E_1 denotes the exponential integral function. The lower limit of integration $l_i(x,y) = l(t_i(x,y))$ denotes the mold position when the deforming SMC front first reaches a given point (x,y) on the mold surface. For points in the initial charge region,

$$l_i = l(0) = l_0. \tag{4.20}$$

Although (4.18) holds for a charge of arbitrary shape, we consider, for purposes of illustration, a rectangular mold cavity charged as shown in Fig. 3. Let

$$l_f = 1\,\mathrm{mm}, \quad s = 0.2\,\mathrm{mm \cdot s^{-1}}. \tag{4.21}$$

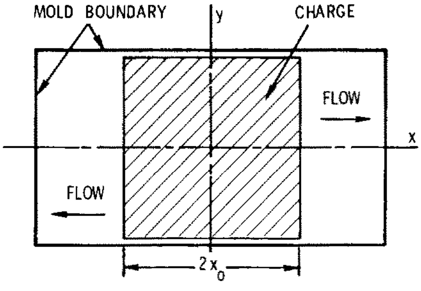

CHARGE PATTERN

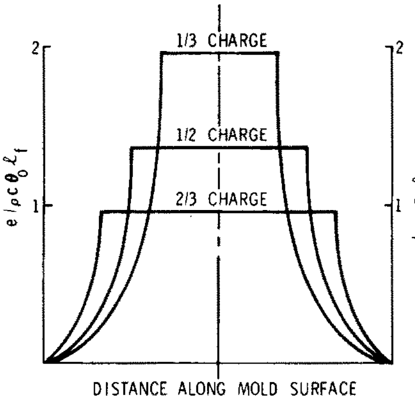

FIG. 3. Heat per unit area absorbed from the mold surface as the mold closes, for three charge fractions.

Then since all quantities are independent of y, an expression for $l_i(x)$ follows directly from (3.4) and (4.20):

$$l_i(x) = \begin{cases} l_0, & x \leqslant x_0, \\ l_0\left(\dfrac{x_0}{x}\right), & x > x_0. \end{cases} \tag{4.22}$$

From (2.1), (4.5), (4.19), and (4.21), we have

$$F = (1.4)\frac{l_0}{l_f}, \tag{4.23}$$

where l_f/l_0 is simply equal to the charged fraction of the mold surface area. Using (4.21) to (4.23), the heat flux integral (4.18) was evaluated for charge fractions of 1/3, 1/2, and 2/3. The results are displayed in Fig. 3. Note that most of the heat is drawn from the charge region of the mold and that the degree of nonuniformity in $e(x)$ diminishes as more of the mold surface is charged.

5. CURE KINETICS

Cure rate equation

Before analyzing heat conduction in the curing compound for $t > t_f$, we first characterize the exothermic cure reaction in the polyester resin.

The reaction kinetics of thermosetting polymers are usually characterized under isothermal conditions. Such a description is useful in the many commercial processes where cure rate is relatively slow compared to the rate of heat conduction in the polymer. But since the polyester resin in SMC cures rapidly at production mold temperatures, the exothermic reaction can strongly couple with heat conduction in the part, causing the resin to cure nonuniformly. The temperature variations that occur in such cases can be highly complex, so that in general we need a description of the thermoset cure reaction which makes no prior assumption on the temperature history.

We follow the work of Kamal *et al.* [4, 5] and characterize the degree of cure in the SMC by the amount of heat evolved by the reaction. Let Q_T be the total amount of heat evolved per unit mass of SMC during the entire reaction, and let Q represent the heat evolved to the present time t. In terms of Q, the degree of cure (or simply the cure) is defined by

$$\alpha = Q/Q_T. \tag{5.1}$$

The cure is a field quantity that varies with material point and time.

At every material point in the SMC, we assume that the rate of cure is specified by a constitutive equation in the form

$$\dot{\alpha} = g(\alpha, T), \tag{5.2}$$

where T is the local absolute temperature. In general, the rate of cure can depend on $\dot{T}$ as well, but this does not appear to be necessary for the present purpose. For constant Q_T, the local rate of heat generation is obtained by combining (5.1) and (5.2) in the form

$$\dot{Q} = Q_T\dot{\alpha} = Q_T g(\alpha, T). \tag{5.3}$$

For stepwise isothermal cure of a similar resin system, Kamal *et al.* [5] use the following form for the cure rate equation (5.2):

$$\dot{\alpha} = (d_1 + d_2\alpha^m)(1-\alpha)^n, \tag{5.4}$$

where m and n are constants and (5.5)

$$d_1 = a_1\,\mathrm{e}^{-b_1/RT}, \quad d_2 = a_2\,\mathrm{e}^{-b_2/RT}.$$

The coefficients a_1, a_2, b_1, and b_2 are constants, and R is the gas constant. In the present analysis, we adopt (5.4) for arbitrary temperature histories.

Determination of the kinetic coefficients

The six constants in the cure rate equation (5.4) can be determined using data from differential scanning calorimetry (DSC) tests. For a description of this apparatus and its use, see [6]. Broadly speaking, the differential scanning calorimeter is used to measure $\dot{Q}$ while the temperature of the material sample is held constant (isothermal mode), or increased at a constant rate (scanning mode).

The pressure in the molded SMC is typically about 7 MPa during cure. Kubota [7] has shown that the cure rate of a polymer resin varies with pressure, but that this effect diminishes above 1 MPa. Therefore, DSC tests on the SMC material considered in this paper were run in a pressurized nitrogen atmosphere† at 4.1 MPa to simulate actual mold conditions as much as possible. Because of the high pressures required, it proved more convenient to operate the DSC in its scanning mode. In this mode, the heat balance for the sample can be written as

$$c\frac{\mathrm{d}T}{\mathrm{d}t} = \dot{Q} + \dot{Q}_l, \tag{5.6}$$

where $\dot{Q}$ is the heat generation rate defined by (5.3) and $\dot{Q}_l$ is the measured rate of heat supplied by the DSC to maintain a constant $\mathrm{d}T/\mathrm{d}t$. Since $\dot{Q}_l$ is measured and the scanning rate $\mathrm{d}T/\mathrm{d}t$ is prescribed, $\dot{Q}$ can be computed from (5.6).

Samples of uncured SMC weighing approximately 30 mg were tested in a DSC at scanning rates of 10, 20, and 50 K·min^{-1}. Figure 4 shows the measured heat generation rate vs temperature for each scanning rate. The total measured heat of reaction Q_T at each scanning rate was approximately 84 J·g^{-1}. Values for the six kinetic parameters were obtained by fitting (5.4) and (5.5) to the DSC data. These values are:

$$\begin{aligned} &a_1 = 4.9\times10^{14}\,\mathrm{s}^{-1}, && b_1 = 140\,\mathrm{kJ\cdot mol^{-1}},\\ &a_2 = 6.2\times10^{5}\,\mathrm{s}^{-1}, && b_2 = 51\,\mathrm{kJ\cdot mol^{-1}},\\ &m = 1.3, && n = 2.7. \end{aligned} \tag{5.7}$$

The theoretical curves obtained by numerical integration of (5.4) and (5.5) using the values (5.7) are also shown in Fig. 4 for comparison.

6. HEAT CONDUCTION AND CURE AFTER MOLD-CLOSING

The temperature distribution developed in the deforming SMC as it fills the mold cavity provides the initial condition for the heat conduction problem that begins once the mold has closed. Since the resin cures during this phase of the molding cycle, it might appear that the details of the curing process depend strongly on convective heat transfer during mold-closing. While this is certainly true in general, considerable simplification is possible for sheet-like parts. To see this, let $\hat{\theta}(x, y, z, \tau)$ represent the developing temperature distribution in a fully molded, uncured sheet starting from the same uniform temperature as the undeformed charge, but at a different time $\tau = 0$. In the early stages of cure, the heat of reaction is negligible and for a slowly varying

---

†This high pressure was also necessary to keep the styrene monomer from evaporating during cure.

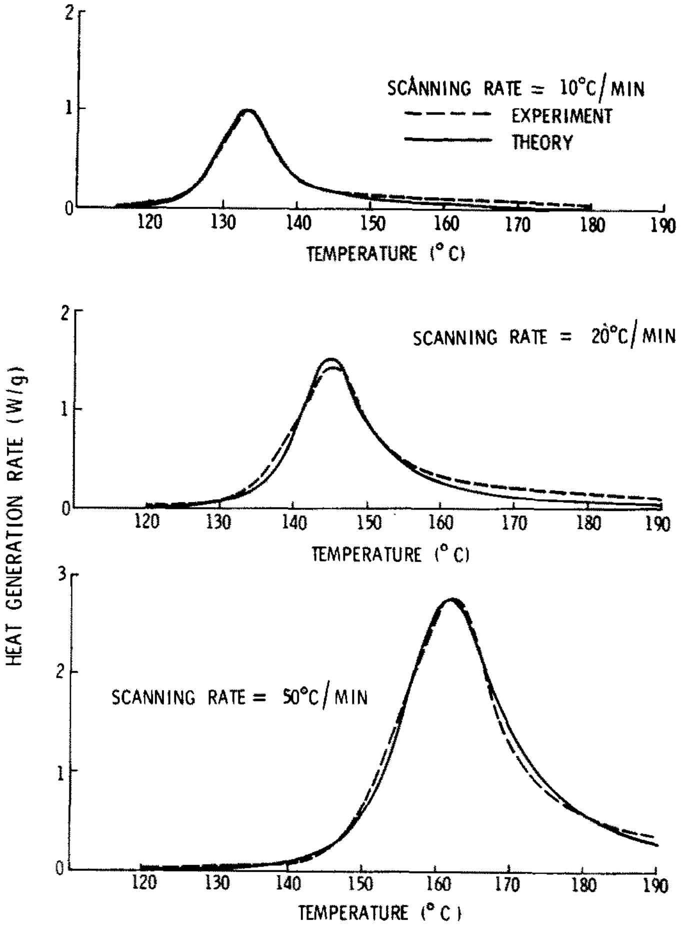

FIG. 4. Heat generation during cure: Comparison of theory and experiment.

part thickness, $\hat{\theta}$ is given approximately by [3, p. 100]

$$\hat{\theta}/\theta_0 = 1+4\sum_{n=0}^{\infty}\frac{(-1)^{n+1}}{(2n+1)\pi} \times \exp\left[\frac{-a_n\kappa_1\tau}{l_f^2(x,y)}\right]\cos\left[\frac{(2n+1)\pi z}{2l_f(x,y)}\right]. \quad (6.1)$$

Since the solutions (4.6) and (6.1) differ only in the argument of the exponential terms, at any point† (x, y), it is always possible, given some t in (4.6), to find a time $\tau = \tau^*(x, y, t)$ in (6.1) such that the respective temperature distributions θ and $\hat{\theta}$ are identical. Let the two temperature distributions coincide at the instant the mold closes $(t = t_f)$. Recalling the transformation (3.14), a simple comparison of (4.6) and (6.1) then gives

$$\tau^*(x, y, t_f) = l_f^2(x, y)f(x, y, t_f). \quad (6.2)$$

Now since the boundary conditions on each problem are the same for $t > t_f$ and for any point (x, y) the two solutions coincide at $t = t_f$, we have

$$\theta(x, y, z, t) = \hat{\theta}(x, y, z, t-(t_f-\tau^*)), \quad (6.3)$$

for

$$t \geqslant t_f. \quad (6.4)$$

Of course, during later stages of cure the heat of reaction is no longer negligible and $\hat{\theta}$ is more involved than (6.1). But since the resin does not begin to cure significantly until after the mold closes, (6.3) implies that the heat transfer in the deforming compound during mold-closing affects conduction and cure after closing only through a time shift $t_f-\tau^*$ on the solution $\hat{\theta}$. From (4.8) and (6.2), the time difference $t_f-\tau^*$ is bounded by

$$0 \leqslant t_f-\tau^* \leqslant t_f. \quad (6.5)$$

To analyze heat conduction in the curing SMC, it is convenient to work in terms of absolute temperature because the cure kinetics of the polyester resin are expressed in terms of absolute temperature. For fixed values of x and y, let T be the absolute temperature field corresponding to $\hat{\theta}$, and let T_0 be the initial temperature of the charge and T_m the temperature of the mold. Then from the result (6.3), we can analyze heat conduction and cure for $t \geqslant t_f$

---

†Note that we have returned to a spatial description of the temperature field because the material no longer deforms after the mold closes.

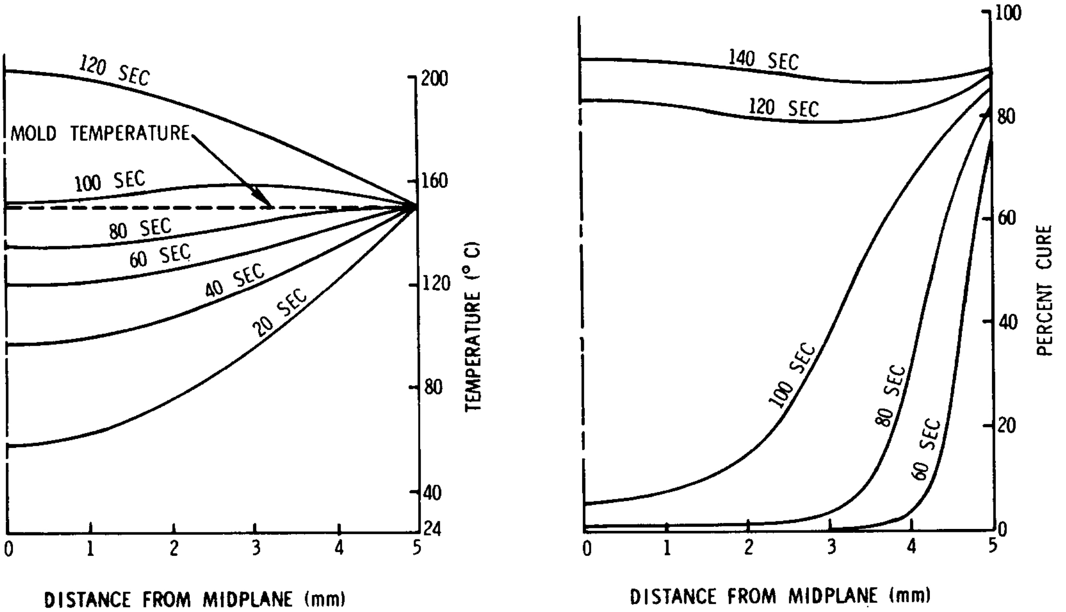

FIG. 5. Temperature and cure profiles for a 10-mm thick sheet.

by considering solutions to the coupled problem:

$$\rho c \frac{\partial T}{\partial \tau} = k_1 \frac{\partial^2 T}{\partial z^2} + \rho \dot{Q}$$

$$\dot{Q} = Q_T[a_1 \exp(-b_1/RT) + a_2 \exp(-b_2/RT)\alpha^m](1-\alpha)^n \qquad (6.6)$$

$$T(x, y, l_f, \tau) = T_m, \quad \frac{\partial T}{\partial z}(x, y, 0, \tau) = 0,$$

$$T(x, y, z, 0) = T_0,$$

where we have used (6.3) to (6.5) and neglected in-plane temperature gradients.

The solution to (6.6) is complicated by the fact that $\dot{Q}$ depends explicitly on the degree of cure and so becomes a path-dependent function of temperature. Consequently, it is not possible to scale the variables such that all solutions of (6.6) can be derived from a single solution in non-dimensional form. Because of the complexity of the expression for $\dot{Q}$, it was necessary to solve (6.6) numerically. The solutions illustrated in the next section were obtained by explicit numerical integration of the corresponding finite difference representation of (6.6).

7. EXAMPLES

Before considering two examples, it is helpful to examine the relative magnitude of terms in the heat balance equations $(6.6)_1$. We first introduce the non-dimensional variables:

$$\sigma = \kappa_1 t/l_f^2, \quad \zeta = z/l_f, \quad \hat{T} = T/\theta_0. \qquad (7.1)$$

Substitution of (7.1) into $(6.6)_1$ yields

$$\frac{\partial \hat{T}}{\partial \sigma} = \frac{\partial^2 \hat{T}}{\partial \zeta^2} + \left(\frac{l_f^2}{\kappa_1 c \theta_0}\right)\dot{Q}. \qquad (7.2)$$

Since d_1 is small relative to d_2 in the expression (5.4) for $\dot{Q}$, the order of magnitude of the last term in (7.2) is

$$\left(\frac{l_f^2}{\kappa_1 c \theta_0}\right)\dot{Q} = O\left(\left[\frac{Q_T}{c\theta_0}\right]\cdot\left[\frac{d_2}{\kappa_1/l_f^2}\right]\right). \qquad (7.3)$$

The degree of coupling between heat generation and heat conduction will depend on the magnitude of (7.3).

The first term in (7.3) expresses the ratio of heat evolved by the reaction to the heat required to raise the temperature of the SMC to that of the mold.† The second term expresses the ratio of the heat conduction time scale (l_f^2/κ_1) to the time scale of the cure reaction $(1/d_2)$. For SMC, the ratio $Q_T/(c\theta_0)$ is $O(1)$ over the range of common mold temperatures. Hence, the degree of coupling between conduction and cure depends only on the ratio of time scales:

$$\nu = \frac{l_f^2/\kappa_1}{1/d_2}. \qquad (7.4)$$

When heat conduction proceeds rapidly relative to the rate of cure, ν is small and coupling is weak. On the other hand, when the reaction proceeds rapidly relative to the rate of thermal diffusion, ν is large‡ and coupling is strong. Both cases are illustrated in the examples that follow.

Thick parts

First consider the interaction of heat conduction and cure in a 10-mm thick sheet when the mold temperature is 150°C. Figure 5 shows temperature and cure profiles in the sheet at equal time intervals.

It is apparent from Fig. 5 that soon after $t = 0$, the material adjacent to the mold surface approaches the

---

† Both quantities are measured per unit mass.

‡ A quantitative indication of what is meant by the comparative terms "small" and "large" is given later in the section.

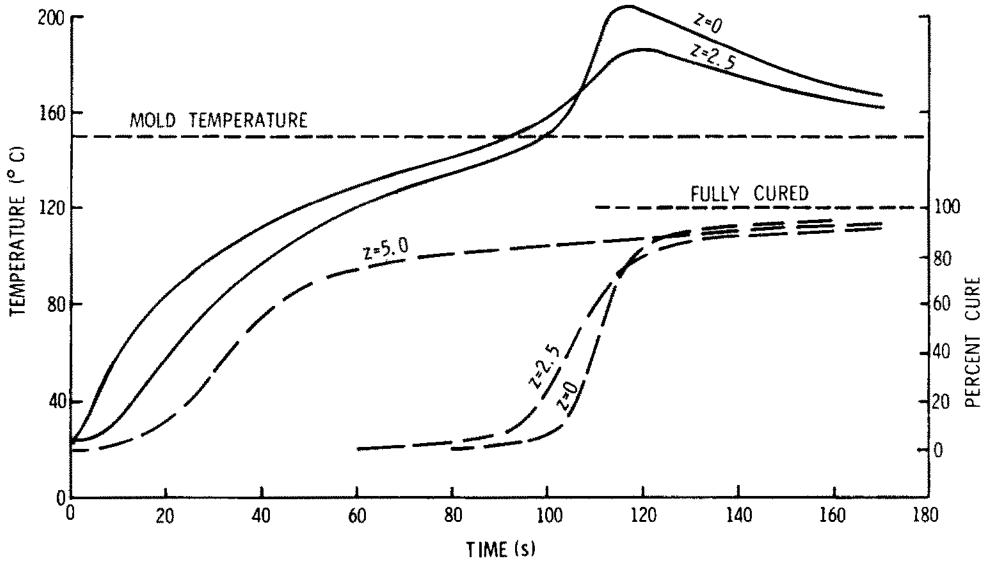

Fig. 6. Temperature and cure vs time at three points in a 10-mm thick sheet.

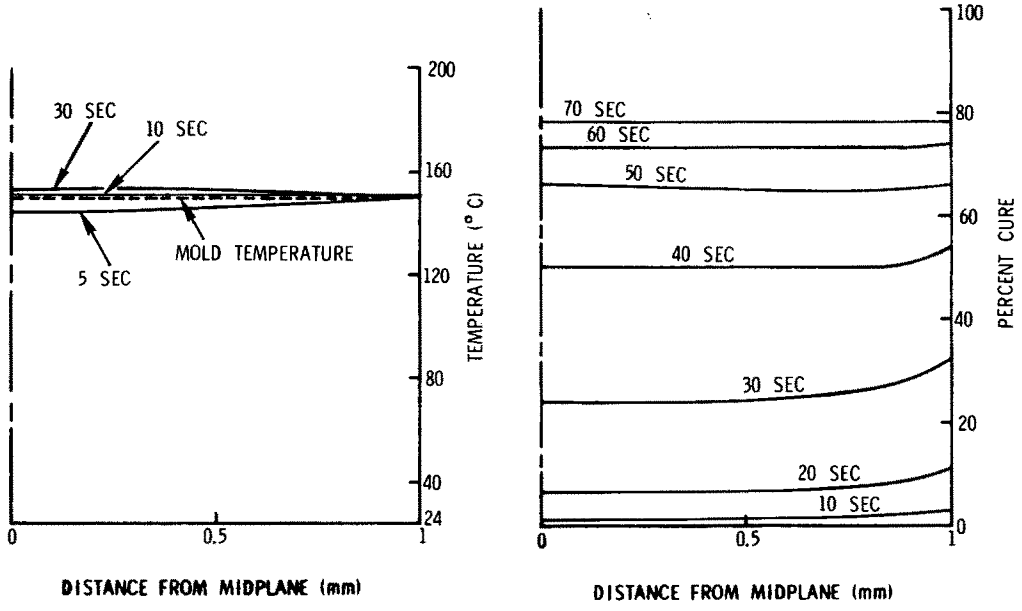

Fig. 7. Temperature and cure profiles for a 2-mm thick sheet.

mold temperature and begins to cure. As the material in this outer region cures, its temperature remains near 150°C because of the proximity of the mold surface. Later, when material closer to the center of the sheet begins to cure, the exothermic heat must diffuse over a greater distance in the SMC to reach the mold. Since this prevents rapid diffusion of heat away from the curing material, the inner region of the sheet increases in temperature as it cures.

As cure progresses toward the center of the sheet, the temperature continues to increase, thereby accelerating the reaction. This can be seen from the increasing separation between successive cure profiles in Fig. 5b. Finally, the cure process culminates in extremely rapid cure of the center region accompanied by a sharp increase in temperature at $t = 120$ s.

A good indication of the nonuniform cure in this example is given by Fig. 6. Here the temperature and cure are plotted as functions of time at the midplane of the sheet ($z = 0$), the mold interface ($z = 5.0$), and at $z = 2.5$. The sudden cure at $z = 0$ together with the rapid and substantial temperature increase at about $t = 110$ s is rather striking.

It is clear from the above discussion that the substantial thickness of the sheet (10 mm) prevents the heat of reaction from diffusing into the mold at the same rate that it is generated. In this example, $\nu \simeq 25$, a value consistent with the strong coupling between heat conduction and cure indicated by the results.

Thin parts

As an example of a relatively thin part, we consider a 2-mm thick sheet in a mold at 150°C. Profiles of temperature and cure for this case are shown in Fig. 7.

In contrast to what is observed in the 10-mm sheet, cure in the 2-mm sheet is virtually uniform. Here, the entire sheet reaches the mold temperature before appreciable cure takes place. Although a substantial amount of heat is generated per unit volume, the temperature in the sheet does not increase significantly. This is because the relatively low thermal resistance of the thin sheet allows the heat of reaction to diffuse into the mold at about the same rate that it is generated. Accordingly, for this case the ratio of time scales ($\nu \simeq 1$) is an order of magnitude less than in the previous example. This is consistent with the weak coupling observed in Fig. 7.

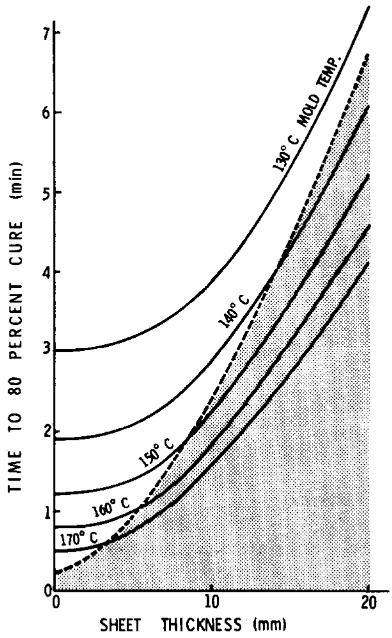

FIG. 8. Cure time versus sheet thickness for various mold temperatures (unshaded region defines admissible molding conditions).

8. CURE TIME

A part can be removed from the mold only after adequate structural properties are developed through sufficient cure of the polymer resin. It is assumed here that this occurs when $\alpha \geqslant 0.8$ everywhere in the part.† Figure 8 summarizes the relationship between cure time and sheet thickness for various mold temperatures. Compression molding of SMC is commonly done near 150°C. Note that for a given mold temperature, thick sheets take longer to cure than thin ones, but since part dimension only affects cure rate indirectly through the coupling of heat conduction and cure, the curves for constant mold temperature flatten at thinner dimensions where this coupling is weak. For very thin parts, cure time depends solely on the reaction kinetics of the polyester resin.

Unlike part dimension, temperature affects the cure rate directly (5.5). This is reflected in Fig. 8 by the fact that as mold temperature is increased, cure time is reduced for all sheet thicknesses. The speed of the process is limited, however, since in the shaded region of Fig. 8, resin temperatures during cure exceed 200°C and the polyester begins to thermally degrade. Hence, molding must be confined to the unshaded region and, for a given cure time, the dashed boundary of the shaded region determines the maximum sheet thickness that can be molded without degrading the resin.

Acknowledgement—We wish to express our gratitude to Ed Herman and Bill Todd of General Motors Manufacturing Development Staff for generously sharing their practical experience in compression molding. Thanks are also extended to Lisa Riley for assisting in the determination of the kinetic coefficients, and to Steve Swarin for performing the DSC tests.

REFERENCES

1. L. F. Marker and B. Ford, Flow and curing behavior of SMC during molding, *Modern Plastics* **54**, 64–70 (1977).
2. D. C. Chang and M. R. Barone, Minimum-weight design in double-layer panels—sheet molding compound vs steel, *Composite Materials: Testing and Design (Fifth Conf.)*, ASTM STP 674, S. W. Tsai, Ed. (1979).
3. H. S. Carslaw and J. C. Jaeger, *Conduction of Heat in Solids*, 2nd edn. Oxford Univ. Press, Oxford (1959).
4. M. R. Kamal and S. Sourour, Kinetics and thermal characterization of thermoset cure, *Polymer Engng Sci.* **13**(1), 59–64 (1973).
5. M. R. Kamal, S. Sourour and M. Ryan, Integrated thermorheological analysis of the cure of thermosets, *SPE Tech. Pap.* **19**, 187–191 (1973).
6. S. Sourour and M. R. Kamal, Differential scanning calorimetry of epoxy cure: isothermal cure kinetics, *Thermochem. Acta* **14**, 41–59 (1976).
7. H. Kubota, Curing of highly reactive polyester resin under pressure: kinetic studies by differential scanning calorimetry, *J. Appl. Polymer Sci.* **19**(8), 2279–2297 (1975).

---

† Experimental evidence exists [6] to show that the degree of cure α, as defined by (5.1), is directly related to the developing stiffness in the curing resin. The choice of $\alpha = 0.8$ is a conservative estimate based on actual molding experience.

EFFET DE LA DEFORMATION ET DE LA RETICULATION THERMIQUE SUR LA CONDUCTION DE LA CHALEUR PENDANT LE MOULAGE D'UN POLYESTER RENFORCE PAR DES FIBRES COURTES

Résumé—On étudie la conduction thermique dans une résine polyester renforcée par des fibres courtes, pendant le moulage par compression de minces plaques. Puisque la résine génère de la chaleur pendant la réticulation, le problème général avec conditions aux limites concerne un conducteur thermique qui se déforme et qui réagit chimiquement. La structure de fibres imbriquées au hasard dans la plaque composite pour moulage (PCM), suggère une hypothèse cinématique sur la déformation du matériau dans la cavité du moule. La description du champ de déformation est ensuite utilisée pour formuler le problème avec conditions aux limites pour la distribution des températures dans la PCM en cours de déformation, en fonction des coordonnées qui se déplacement dans le matériau. A partir de la solution de ce problème, on obtient une expression générale analytique pour la distribution non uniforme de la chaleur absorbée à la surface du moule. La réaction exothermique de réticulation dans la résine, commençant à la fermeture du moule, est caractérisée en fonction de la chaleur créée dans la PCM. L'analyse numérique de la distribution transitoire de température et du degré de réticulation montre que le couplage entre la conduction thermique et la réticulation dépend de l'épaisseur de la plaque à mouler. Les résultats de l'analyse détermine l'effet de l'épaisseur de la plaque et de la température du moule sur le temps de réticulation, compte tenu des limitations de la dégradation thermique.

DER EINFLUSS VON VERFORMUNG UND WÄRME-AUSHÄRTUNG AUF DIE WÄRMELEITUNG IN EINEM MIT KURZEN GLASFASERN VERSTÄRKTEN POLYESTERHARZ WÄHREND DES FORMPRESSENS

Zusammenfassung—Diese Arbeit behandelt die Wärmeleitung in einem mit kurzen Glasfasern verstärkten Polyesterharz während des Formpressens von dünnen, schichtförmigen Teilen. Da das Harz während des Aushärtens Wärme erzeugt, stellt das allgemeine Randwertproblem einen sich verformenden Wärmeleiter dar, der chemisch reagiert. Aus der zufallsorientierten Faserstruktur in der Schichtformungsmasse (SFM) läßt sich eine Annahme über die Kinematik der Materialverformung im Formhohlraum treffen. Die resultierende Beschreibung des Deformationsfeldes wird dann benutzt, um das Randwertproblem für die Temperaturverteilung in der SFM in Abhängigkeit von Koordinaten zu formulieren, die sich mit dem Material bewegen. Aus der Lösung dieser Aufgabe leiten wir in geschlossener Form einen allgemeinen Ausdruck ab für die ungleichförmige Verteilung der Wärmeaufnahme durch die Oberfläche der Form bei der Pressung eines jeden Teils. Die exotherme Aushärtungsreaktion des Polyesterharzes, die nach dem Schließen der Form beginnt, wird durch Wärmequellen in der SFM beschrieben. Die numerische Berechnung der instationären Verteilung von Temperatur und Aushärtung zeigt, in welchem Maße die Kopplung zwischen Wärmeleitung und Aushärtung von der Schichtdicke abhängt. Die Ergebnisse der Untersuchung geben ebenfalls Aufschluß über den Einfluß von Schichtdicke und Formtemperatur auf die Aushärtezeit, die ihrerseits durch thermischen Abbau begrenzt ist.

ВЛИЯНИЕ ДЕФОРМАЦИИ И ТЕРМИЧЕСКОГО ОТВЕРЖДЕНИЯ НА ТЕПЛОПРОВОДНОСТЬ НАПОЛНЕННОГО ОТРЕЗКАМИ ВОЛОКНА ПОЛИЭФИРА ПРИ ФОРМОВКЕ ПОД ДАВЛЕНИЕМ

Аннотация—В статье рассматривается теплопроводность полиэфирной смолы, наполненной отрезками волокна, при формовке из них под давлением изделий в виде тонких пластин. Поскольку отверждение сопровождается тепловыделением, в общей граничной задаче учитывается теплопроводность деформируемого материала, принадлежащего к химически активным веществам. Хаотическое расположение волокон в листовом изделии оправдывает кинематическое допущение о деформации материала в полости прессформы. Такое описание поля деформации используется затем для формулировки краевой задачи о распределении температур в координатах, связанных с деформируемым материалом. Решение даёт в замкнутом виде общее выражение для неоднородного распределения тепловой энергии, выделяемой каждой частью поверхности изделия при формовке. Экзотермическая реакция отверждения полиэфирной смолы, начинающаяся с момента закрытия прессформы, характеризуется интенсивностью тепловыделений. Численный анализ нестационарного температурного поля при отверждении устанавливает взаимосвязь между потоком теплопроводности и характеристиками твердения и обнаруживает зависимость от толщины изделия. В результате определено также влияние толщины и температуры формуемого изделия на время отверждения при условии наложения ограничений на термическую деструкцию.